A computational method of prediction of the end-diastolic pressure–volume relationship by single beat

Stefan Klotz[1], Marc L Dickstein[2] & Daniel Burkhoff[3]

[1]Department of Thoracic and Cardiovascular Surgery, University Hospital, Muenster, Germany. [2]Department of Anesthesiology, College of Physicians and Surgeons, Columbia University, New York City, New York 10032, USA. [3]Department of Medicine, College of Physicians and Surgeons, Columbia University, New York City, New York 10032, USA. Correspondence should be addressed to S.K. (Stefan.Klotz@ukmuenster.de).

Published online 30 August 2007; doi:10.1038/nprot.2007.270

The end-diastolic pressure–volume relation (EDPVR) is an important descriptor of passive cardiac pump properties. However, clinical utility has been limited by the need for measurement of pressures and volumes over relatively large ranges. In this protocol, we describe an algorithm to estimate the entire EDPVR in humans from a single measured pressure–volume (P–V) point. This algorithm was developed from observations made from accurately measured EDPVRs of human hearts, which indicated that when normalized by appropriate left ventricular volume scaling (to arrive at volume-normalized EDPVRs, $EDPVR_n$) $EDPVR_n$s were nearly identical in all patients. In this protocol, we demonstrate how to use $EDPVR_n$s to predict a second P–V point on the EDPVR, in which case the entire EDPVR can then be predicted. With recent advances for accurate noninvasive measurement of end-diastolic pressure and volumes, this protocol permits the assessment of passive properties in a broader range of research and clinical settings.

INTRODUCTION

The end-diastolic pressure–volume relationship (EDPVR) is one of the most important means of characterizing the passive ventricular properties of an individual heart. In particular, the EDPVR indicates the physiologic determinant of preload by indicating the amount of diastolic filling that will occur for a specified filling pressure[1,2]. In addition, assessment of this relationship is fundamental to the study of ventricular remodeling in heart failure, and especially to study the effect of surgical, pharmacologic or device-based treatment strategies on reverse remodeling[3–6].

The most accurate measurement of EDPVRs in human and animal hearts is performed *ex vivo* in a straightforward manner by placing a volume-compliant balloon into the left ventricle (LV) of the heart; volume is then varied by a calibrated syringe while pressure is measured[7–9]. Because this is an artificial setting, volumes and pressures can easily be varied over wide ranges for direct assessment of the EDPVR over extended physiologic range. In contrast, *in vivo* assessment of the EDPVR requires use of a means of continuous pressure and volume measurement, such as a conductance catheter or multidimensional sonomicrometry, over a range of pressures and volumes induced by transient inferior vena cava occlusion (IVCO)[10,11]. Since sonomicrometry is not feasible in humans, the conductance catheter technique is the only practical technique that can be used for this purpose. However, this technique is very invasive. In addition, the need of transient vena cava occlusion requires additional instrumentation of the patient and is not a familiar procedure to a majority of clinical investigators. Thus, widespread use of this technique is limited by the invasiveness of this procedure and the need for highly specialized equipment.

In recent years, noninvasive techniques for the measurement of ventricular pressures and volumes became available. Some approaches that continue to evolve for these measurements include Doppler-echocardiography[12–15], radionuclide ventriculography[16,17] and MRI[18]. The utility of these approaches will become more and more evident, because it obviates the need to perform an IVCO to define the EDPVR.

Similar to the relatively precise and useful approach for estimation of the entire end-systolic pressure–volume relationship (ESPVR) from end-systolic pressure and volume measured from a single beat[19–21], recently we were able to generate and validate a method for predicting the entire EDPVR from a single measured end-diastolic pressure–volume point[22]. With this publication, we want to make our approach widely available so that others may embark on this technique.

Algorithm

This single-beat EDPVR estimation algorithm is based on the premise that the EDPVR can generally be described by a common nonlinear analytical expression with coefficient values that are reasonably well linked with the size of the heart[23]. This suggests that overall these EDPVRs share a common underlying shape. The present algorithm is intended to facilitate the use of EDPVR in clinical and research settings in humans and animals where assessment of changes in passive ventricular properties are important, such as in certain disease states and after therapeutic interventions.

Despite large differences in sizes and geometries, EDPVRs of hearts of different species (human, canine, rat) in normal or diseased states can all be described by common nonlinear analytical expressions, such as $EDP = \alpha \cdot EDV^{\beta}$ or $EDP = \alpha \cdot e^{\beta \cdot EDV}$, with different coefficient values represented by α and β[23]. This suggests that EDPVRs of different species and disease states may share a common underlying shape. In all species and states of health, EDPVRs generally span the same and relatively limited range of pressures, from 0 mmHg to a maximum of 30 or 40 mmHg. The major difference in the EDPVRs of such different hearts is the range over which volume varies to achieve this same range of pressures. All these features suggested that if an appropriate method of scaling ventricular volume could be arrived at and was used to normalize volumes, we could arrive at a volume-normalized EDPVR ($EDPVR_n$) that would be very similar for the hearts of different species and states of health.

To test this hypothesis, in our recent paper[22] we reported the measurement of *ex vivo* EDPVRs from human and rat hearts where we normalized ($EDPVR_n$) in the volume dimension to account for the unstressed volume (V_0, volume at which EDP is approximately

0 mmHg) and V_{30}, the volume in milliliter at which EDP equals 30 mmHg, according to the following equation:

$$\mathrm{EDV}_n = \frac{(\mathrm{EDV} - V_0)}{(V_{30} - V_0)} \quad (1)$$

Representative examples of EDPVRs measured from *ex vivo* human and rat hearts are shown in **Figure 1**. As shown in these examples, EDPVRs from different types of hearts and different diseases spanned very wide ranges of volumes. Some hearts reached filling pressures of 30 mmHg at as little as approximately 80 ml and other reached this same pressure at more than 300 ml. In the rat hearts, the same filling pressures were reached with a volume of 0.4–0.8 ml. These same EDPVRs are shown in **Figure 2** after volumes were normalized according to Equation 1. As suggested, the curves revealed a high degree of concordance. **Figure 3** shows data from all human EDPVR$_n$s superimposed on each other to visually determine their degree of similarity. As shown, there is relatively little deviation of these normalized data around a common curve and could be described well by the equation:

$$\mathrm{EDP} = \mathrm{A}_n\mathrm{EDV}_n^{Bn} \quad (2)$$

where values for EDP are in mmHg, EDV in milliliter, A_n in mmHg and B_n is unitless. Optimal A_n and B_n values (± SD) obtained from the group of human hearts as a whole were 27.78 ± 0.3 mmHg and 2.76 ± 0.05 (unitless), respectively.

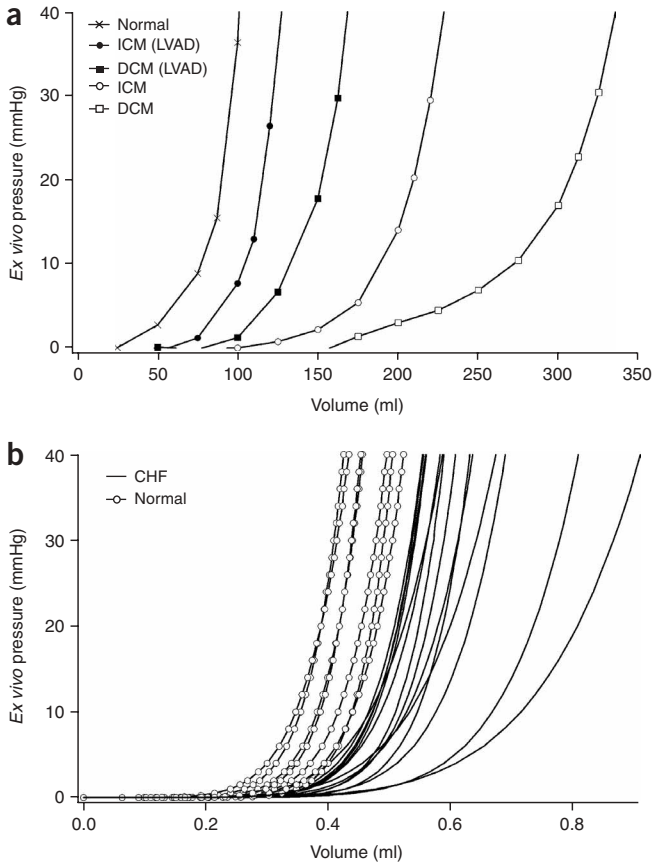

Figure 1 | Examples of end-diastolic pressure–volume relations (EDPVRs). Measured from (**a**) *ex vivo* human hearts and (**b**) *ex vivo* rat hearts. These EDPVRs spanned very wide ranges of volumes from as little as approximately 0.4 ml to greater than 300 ml at filling pressures of 30 mmHg. Used with permission from ref. 22. ICM, ischemic cardiomyopathy; DCM, idiopathic dilated cardiomyopathy; LVAD, hearts supported with a left ventricular assist device.

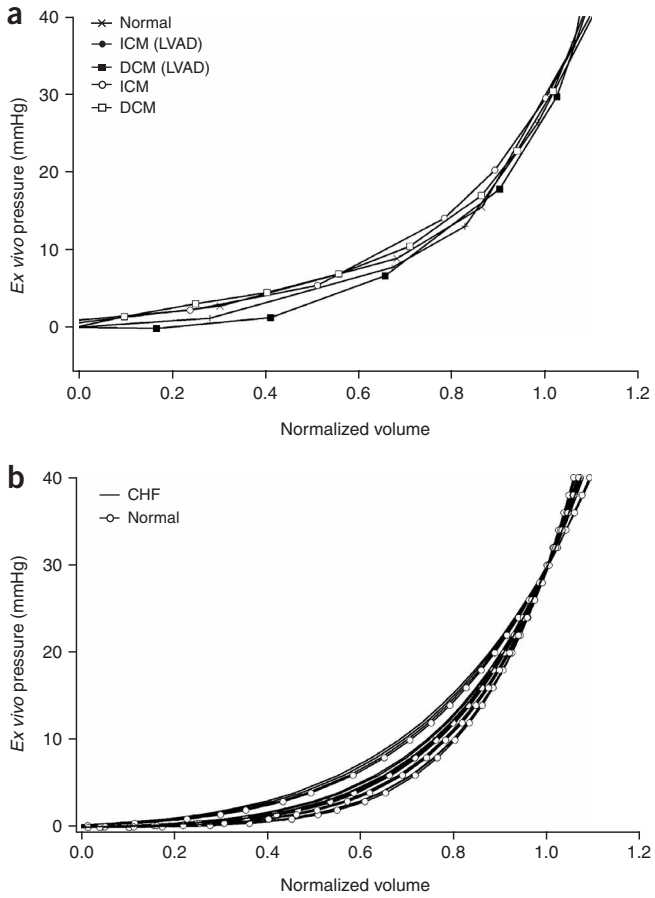

Figure 2 | The same end-diastolic pressure–volume relations (EDPVRs) from **Figure 1** normalized to volume and superimposed on each other. Measured from (**a**) *ex vivo* human hearts and (**b**) *ex vivo* rat hearts. Despite different diseases and different heart sizes, the volume-normalized shape of the curves is the same. Used with permission from ref. 22.

After establishing that Equations 1 and 2 resulted in EDPVR$_n$s in a variety of hearts with a common set of parameter values, our strategy was to devise a means of using the common EDPVR$_n$ and EDP and EDV measured from a single beat to ascertain values of α and β in the equation:

$$\mathrm{EDP} = \alpha\mathrm{EDV}^{\beta} \quad (3)$$

to optimally predict the original EDPVR. This, in turn, was based on a strategy to estimate values of V_0 and V_{30} to insert into Equation 1.

The overall approach, presented in more detail in the following paragraphs, relies on a few key analytical relations and empiric assumptions:

Begin with the measurement of EDP and EDV on a single beat (P_m in mmHg and V_m in milliliter, respectively). These values can be measured invasively (e.g., with conductance catheter) or non-invasively (e.g., echocardiographic volume measurement, Doppler estimation of left atrial pressure based on pulmonary vein flow velocity or E to E′ measurements derived with tissue Doppler echocardiography).

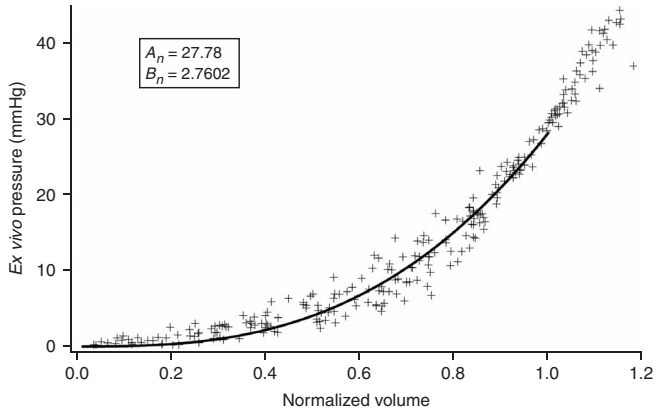

Figure 3 | All *ex vivo* human volume-normalized end-diastolic pressure–volume relation (EDPVR) data shown superimposed on each other revealing an A_n value of 27.78 and a B_n value of 2.76. Used with permission from ref. 22.

Based on Equation 1, normalized measured volume ($V_{m,n}$, unitless number) is defined as follows:

$$V_{m,n} = \frac{(V_m - V_0)}{(V_{30} - V_0)} \quad (4)$$

The resulting $V_{m,n}$–P_m point would fall on the curve:

$$P_m = A_n V_{m,n}^{Bn} \quad (5)$$

Solving Equation 5 for $V_{m,n}$, substituting the result into Equation 4 and solving for V_{30} (in milliliter) yields:

$$V_{30} = V_0 \frac{(V_m - V_0)}{\left(\frac{P_m}{A_n}\right)^{(1/Bn)}} \quad (6)$$

Thus, to predict the EDPVR, a reasonable estimate of V_0 is required. The relative constancy of the shape of the normalized EDPVR suggested a relatively consistent relationship between the volume at a certain pressure and V_0. To test this, we determined the volumes from human *ex vivo* hearts that provided pressures of 10, 15, 20 and 25 mmHg. These volumes designated V_{10}, V_{15}, V_{20} and V_{25}, respectively, where each separately plotted versus the V_0 determined from each measured EDPVR (**Fig. 4**). For each plot, we determined the linear regression equation forced through the origin:

$$V_0 = kV_m \quad (7)$$

The value of k (a unitless constant) obtained at each pressure level was then plotted as a function of P_m, and linear regression analysis was applied with the following result:

$$k = 0.6 - 0.006P_m \quad (8)$$

Substitution of Equation 8 into Equation 7 yields:

$$V_0 = V_m(0.6 - 0.006P_m) \quad (9)$$

We previously showed that the correlation between measured and predicted V_0 using this method was nearly equal to the line of identity with a correlation coefficient of 0.92 (Fig. 5A of ref. 22). In addition, we further showed that the shape and position of the predicted EDPVR is not influenced greatly unless large errors are made in the prediction of V_0 (ref. 22). The entire EDPVR of an individual heart can then be predicted from the analytical determination of α and β for Equation 3 to force the curve through the measured point on the EDPVR and the predicted V_0 (Equation 9) and V_{30} (Equation 6) according to the following:

$$\beta = \frac{\left\{\mathrm{Log}\left(\frac{P_m}{30}\right)\right\}}{\left\{\mathrm{Log}\left(\frac{V_m}{V_{30}}\right)\right\}} \quad (10)$$

$$\left[\alpha = \frac{30}{V_{30}^{\beta}}\right] \quad (11)$$

After establishing the validity of this approach from the data obtained from *ex vivo* human hearts, we prospectively applied the approach to compare the EDPVRs measured from human hearts *in vivo*, normal and failing canine hearts *in vivo* and normal and failing rat hearts *in vivo* and *ex vivo*[22]. In these studies, we examined P_m values ranging up to approximately 25 mmHg.

It was realized that when P_m approaches 30 mmHg, a singularity is encountered in Equation 11, and the value for α becomes indeterminate. To overcome this singularity, we derived an alternate set of equations that calculate values of α and β based on the predication of V_{15} (EDV to achieve a pressure of 15 mmHg) instead of V_{30}, which is based on simple analytical calculations (no further assumptions required).

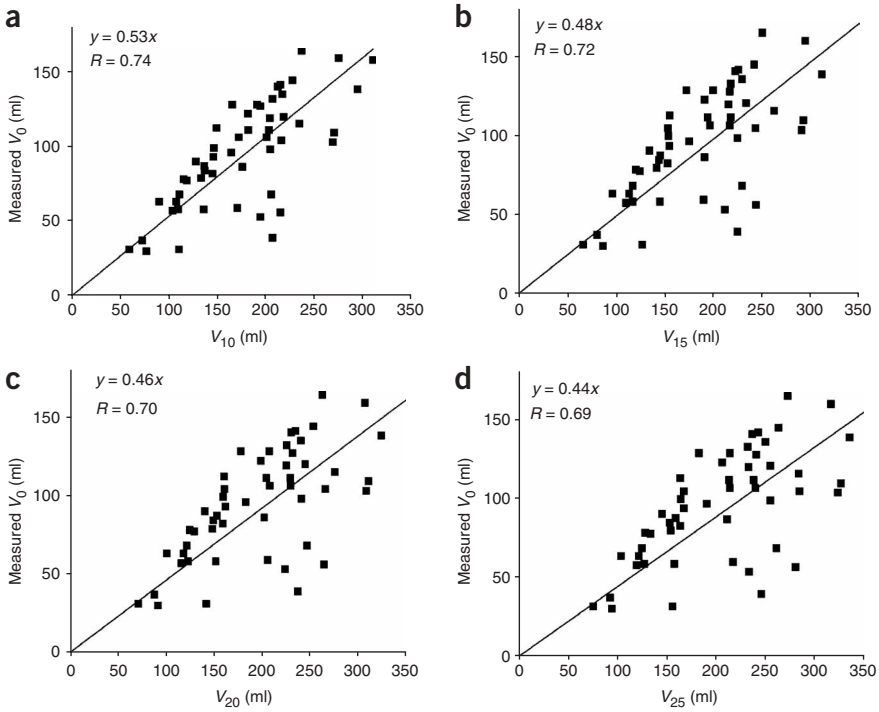

Figure 4 | V_0 measured from human hearts as a function of volume. Filling pressures of (**a**) 10 mmHg (V_{10}), (**b**) 15 mmHg (V_{15}), (**c**) 20 mmHg (V_{20}) and (**d**) 25 mmHg (V_{25}) as shown in the respective panels. Slopes of regression lines shown in each panel. The slope (k) was then plotted as a function of the respective filling pressure to yield the result that, on average, $V_0 \approx V_m(0.6 - 0.006P_m)$. Used with permission from ref. 22.

Based on the equation for the universal EDPVR$_n$, it is analytically determined that the V_n that provides a pressure of 15 mmHg equals 0.8 (see **Fig. 3**). From this fact, we can calculate V_{15} as follows:

$$V_{15} = 0.8(V_{30} - V_0) + V_0 \quad (12)$$

Then, similar to Equations 10 and 11, the entire EDPVR of an individual heart can be predicted from the analytical determination of α and β to force the curve through the measured point on the EDPVR and the predicted V_0 (Equation 9) and V_{15} (Equation 12) according to the following equation:

$$\beta = \frac{\left\{\mathrm{Log}\left(\frac{P_m}{15}\right)\right\}}{\left\{\mathrm{Log}\left(\frac{V_m}{V_{15}}\right)\right\}} \quad (13)$$

$$\alpha = \frac{P_m}{V_m^{\beta}} \quad (14)$$

Equation 13 has a singularity when P_m approaches 15 mmHg. Thus, it is recommended to use Equations 10 and 11 when $P_m \leq 22$ mmHg, and to use Equations 13 and 14 when $P_m > 22$ mmHg. However, in the range between 15 and 22, the EDPVRs predicted from these two sets of equations are essentially the same (see PROCEDURE).

Methods used to obtain data in our proof of principle paper

The foundation of this approach was established in the studies of *ex vivo* human hearts as described in detail previously[22]. In brief, human hearts obtained at the time of cardiac transplantation were obtained for this study. Hearts were from normal subjects not suitable for transplantation, transplant patients with cardiomyopathy and with end-stage cardiomyopathy supported with a LV assist device (LVAD, TCI HeartMate, Thoratec Corp., Pleasanton, CA). Hearts were perfused with cold cardioplegia solution at the time of explant. The aortic root and, in case of the LVAD-supported hearts, the LVAD inflow cannula were clamped occluded. A metal adapter was attached to the mitral annulus and a compliant water-filled latex balloon was placed within the LV chamber. Pressure within each balloon was measured with a high-fidelity micromanometer as volume was progressively increased. The pressure was then plotted as a function of volume at each step. All data were recorded with the data acquisition program Chart 5.1 (ADInstruments Inc., Colorado Springs, CO).

In vivo human experiments

Single-beat estimation of EDPVR was tested using the data obtained from *in vivo* human hearts of normal patients and patients with heart failure. The *in vivo* EDPVRs were assessed by conductance catheter technique using transient IVCO as described in detail previously[19,20].

Animal experiments

Data were also obtained from *in vivo* open chest dogs and chronically instrumented awake dogs in a normal state in following induction of heart failure by repeated coronary microembolization. All animals were instrumented with an indwelling pressure gauge (Konigsberg, CA), sonomicrometer crystals and a balloon occluder around the IVC as described previously[24].

In addition, data were obtained from normal rats and in rats with experimentally induced heart failure state. For *in vivo* assessment of the EDPVR, a Millar conductance catheter (Millar Instruments, Houston, TX) and the technique of IVCO was used. For *ex vivo* assessment, a thin latex balloon was inserted into the LV and LV pressure was measured using a 5-F Millar micromanometer as volume was infused into the balloon at 0.025-ml increments.

MATERIALS

REAGENTS

A single end-diastolic pressure–volume point from the LV of the heart of any species (see REAGENT SETUP) **! CAUTION** All procedures involving human hearts must conform to National and Institutional regulations. Our initial work was approved by the Institutional Review Board of Columbia University (*ex vivo* human experiments) and the John Hopkins Medical Institutions (*in vivo* human experiments). **! CAUTION** All experiments involving animals must conform to National and Institutional regulations. The animals used in our initial work received humane care in compliance with the Guide for the Care and Use of Laboratory Animals published by the National Institutes of Health (NIH publication No. 85-23, revised 1996). All animal studies were approved by the Institutional Animal Care and Use Committee of Columbia University.

EQUIPMENT

Any commercially available computational and scientific graphing program, see EQUIPMENT SETUP.

REAGENT SETUP

Single end-diastolic pressure–volume point from the LV of the heart of any species. The algorithm requires as input the measured EDV and EDP form the LV. EDV and EDP can be measured invasively with pressure catheters, sonomicrometry of conductance catheter, or noninvasively, for example, by Doppler-echocardiography or magnet resonance tomography as described in the INTRODUCTION. Our procedure was evaluated in *ex vivo* in human heart, and tested afterward in human subjects and a rat and canine model (see the section entitled Methods used to obtain data in the INTRODUCTION and ref. 22). The algorithm has been shown to apply equally to hearts of normal subjects (animals or humans) or in subjects with different diseases, such as systolic or diastolic heart failure. This protocol might have limitations in subjects with pericardial constraints. **! CAUTION** Invasive or noninvasive measurements for using this algorithm in human subjects for research purposes require approval by the appropriate Human Subjects Ethics Committee or Institutional Review Board. In addition, experiments on animals should be approved by the appropriate Institutional Animal Care and Use Committee.

EQUIPMENT SETUP

Graphing program Any commercially available computational and scientific graphing program. We used for our analysis IgorPro 4.01 (WaveMetrics Inc., Lake Oswego, OR) but any other analysis environment that can be programmed to compute the output of analytical equations from specified parameters can be used (e.g., Matlab, The MathWorks Inc., Natick, MA or Microsoft EXCEL, Microsoft Corp, Seattle, WA).

PROCEDURE

Subjects

1| Obtain informed consent following the established institutional guidelines.

Obtain measurements

2| Measure a single set of P_m (EDP measured) and V_m (EDV measured) either by invasive or noninvasive means.

Calculations

3| Calculate V_0 from Equation 9.

4| Calculate V_{30} from Equation 6, with A_n value of 27.78 mmHg and B_n value of 2.76.

5| At this stage, two options are available for determining the entire EDPVR; option A allows determination of the EDPVR for measured P_m values up to 22 mmHg, whereas option B allows determination of the EDPVR for measured P_m values above 22 mmHg.

(A) Determining EDPVR for measured P_m up to 22 mmHg

(i) Calculate β from Equation 10.

(ii) Calculate α from Equation 11.

(B) Determining EDPVR for measured P_m over 22 mmHg

(i) Calculate V_{15} from Equation 12.

(ii) Calculate β from Equation 13.

(iii) Calculate α from Equation 14.

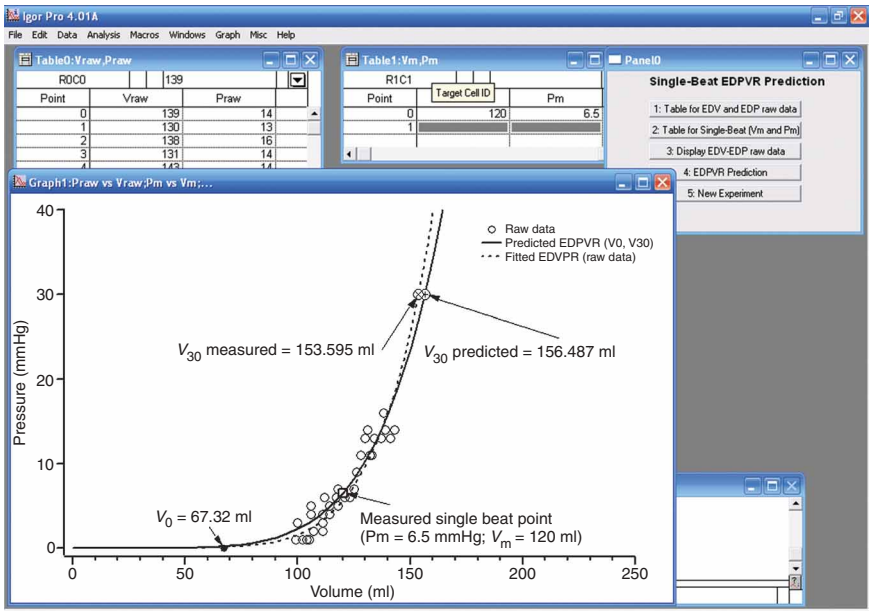

Figure 5 | Final screen of the analyzing computer program IgorPro (see text for details).

6| Use the estimates of α and β to specify the entire EDPVR by $EDP = \alpha EDV^{\beta}$. The complete algorithm is available in a **Supplementary Tutorial**.

ANTICIPATED RESULTS

A representative screenshot from the analyzing program is shown in **Figure 5**. The overall accuracy of this approach to predict V_{30} (Equation 6) is generally very high. As shown in **Figure 6**, the measured versus predicted V_{30} points fall nearly on the line of identity over the large range of volumes tested, indicating a good correlation ($r^2 = 0.98$; $P < 0.001$). The predictive power of the algorithm and the overall general applicability of this approach were tested prospectively using the data obtained from *in vivo* human and animal studies, using the A_n and B_n values obtained from the *ex vivo* human experiments. For these tests, the baseline values of EDP–EDV (i.e., values obtained before the start of IVCO) were the designated P_m and V_m values for EDPVR prediction. Representative examples from human and rat data are shown in **Figure 7**. With the same parameter values for A_n and B_n, the accuracy of predictions were nearly identical despite marked difference in heart size.

An extensive quantitative analysis was performed to define the accuracy with which this approach was able to predict the EDPVR in the different experimental settings (summarized in **Table 1**). *Ex vivo* studies in rat and human hearts yielded nearly identical values of A_n and B_n. Also shown in **Table 1** are the average (±SD) values for the root mean square error (RMSE) differences between measured and predicted EDPVRs in different settings. As seen in **Table 1**, on average, the measured and predicated EDPVRs deviated by a maximum of only 3 mmHg.

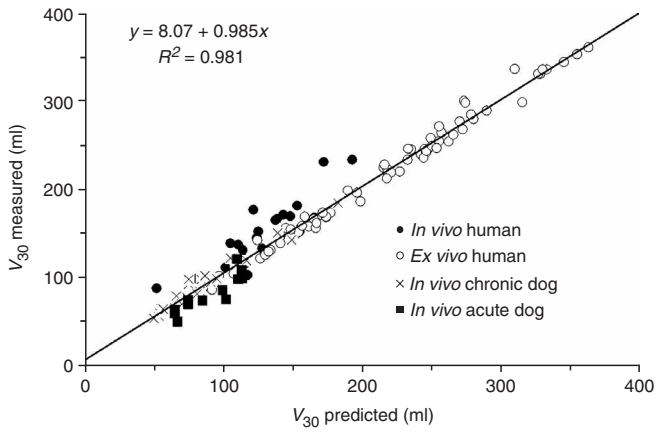

Figure 6 | Correlation plots of the agreement between measured and predicted V_{30}. Used with permission from ref. 22.

Interestingly, though developed primarily based on the data from human hearts, the approach appears to be generally applicable to normal and diseased hearts of different species. Values of RMSE ranging between 0.5 and 6 mmHg among all these hearts indicate that on average the predicted EDPVR falls within 1.8 mmHg of the actual EDPVR over a range of conditions.

The LV EDPVR can be reasonably estimated from a single pressure–volume point, and the predicted relationships are generally well correlated with directly measured data. The results obtained are most accurate when applied to groups of hearts rather than to individual hearts. This new and novel method could enhance the utility of using the EDPVR in clinical and research settings where assessment of the differences in passive ventricular properties between groups of patients or assessing changes in such properties in response to interventions were performed. The potential for noninvasive application is particularly appealing and is complementary to the recently proposed approach to single-beat estimation of the ESPVR.

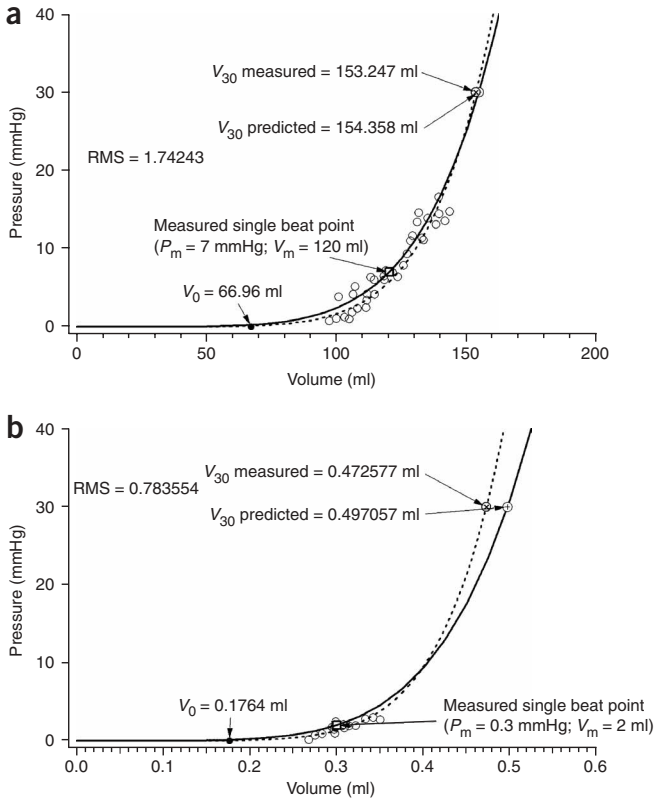

Figure 7 | Two examples of the single-beat estimation of the entire end-diastolic pressure–volume relation (EDPVR). From (**a**) *in vivo* human and (**b**) *in vivo* rat data. Overall, a high prediction capability was observed with the same equation and parameter values from the human hearts, despite different species and heart sizes. The small open circles show the end-diastolic pressure–volume points measured from the *in vivo* human hearts. The large open square shows the end-diastolic pressure–volume point selected for prediction. The dotted line shows the curve fit from the raw data using a nonlinear analytic expression. The solid line shows the entire EDPVR with parameter values predicted from Equation 2. Used with permission from ref. 22.

TABLE 1 | A_n and B_n values derived from each experimental setting along with root mean square error values and correlation coefficient between measured and predicted V_{30}. All values are mean ± SD.

	A_n (mmHg)	B_n (unitless)	RMSE (mmHg)	R^2 (V_{30})
Ex vivo human	27.8	2.76	1.74 ± 1.19*	0.99546
Ex vivo rat	28.3	2.67	1.76 ± 0.79*	0.99786
In vivo human			2.99 ± 1.72	0.89058
In vivo chronic dog			3.02 ± 1.44	0.97833
In vivo acute dog			1.07 ± 0.65*	0.88961
In vivo rat			1.02 ± 0.66*	0.96741

RMSE, root mean square error in the estimate of pressures.*$P < 0.05$ versus *in vivo* human and chronic dog.

Limitations

This protocol in experimental *ex vivo* settings offer ideal conditions in which confounding factors (e.g., controlling respiration) are minimized and volumes and pressures can be varied over a broad range. The values of A_n and B_n were obtained from normal and dilated idiopathic and ischemic cardiomyopathic hearts. This may limit the applicability of the approach to other disease states. Nevertheless, the approach appeared to apply well *in vivo* to patients that have different cardiac disease states (e.g., heart failure and normal ejection fraction due to hypertensive and/or idiopathic hypertrophic cardiomyopathies). This again speaks to the general applicability of the underlying observation that the EDPVR generally has a common shape. Special considerations should be given to the effects of right-sided filling pressures, pericardial pressures and ventricular interdependence. This is especially important in the data generated by caval occlusion in which these pressures are changing and can influence the resulting EDPVR. Although such effects can be eliminated in the studies performed *ex vivo* (i.e., by completely unloading the right ventricle), these effects are difficult (sometimes impossible) to discern *in vivo* without the use of special instrumentation (e.g., pericardial pressure measurements). However, even when measured invasively with a conductance catheter or by sonomicrometry, interpretation of an EDPVR measured *in vivo* during caval occlusion is subject to these same limitations.

In addition, this analysis was not tested in noninvasively acquired pressure–volume points (e.g., by echocardiography), and caution should be taken with implementing this analysis uncritically; validation of specific techniques of predicting the EDPVR from noninvasively estimated P_m and V_m should be undertaken in the future. In our previous study, we also provided a sensitivity analysis showing the degree to which the prediction would be influenced by inaccuracies in measurement of EDPs and EDVs[22]. In the end, the concordance of the prediction to the real EDPVR can only be as good as the measurements of P_m and V_m.

Finally, the present analysis has focused on confirming the accuracy of the ability of this algorithm to predict pressures at various EDVs, or estimation of capacitance (i.e., volumes required to achieve certain pressures). Frequently, however, there is interest to quantify diastolic compliance, which is the slope of the EDPVR. Because the EDPVR is nonlinear, compliance varies with the degree of filling. The algorithm described in this procedure has not been validated for quantifying compliance, which may require a prediction with a significantly greater degree of accuracy.

Note: Supplementary information is available via the HTML version of this article.

COMPETING INTERESTS STATEMENT The authors declare no competing financial interests.

Published online at http://www.natureprotocols.com
Reprints and permissions information is available online at http://npg.nature.com/reprintsandpermissions

1. Jacob, R. & Kissling, G. Ventricular pressure-volume relations as the primary basis for evaluation of cardiac mechanics. Return to Frank's diagram. *Basic Res. Cardiol.* **84**, 227–246 (1989).
2. Sagawa, K. The end-systolic pressure-volume relation of the ventricle: definition, modifications and clinical use. *Circulation* **63**, 1223–1227 (1981).
3. Kass, D.A. *et al.* Reverse remodeling from cardiomyoplasty in human heart failure. External constraint versus active assist. *Circulation* **91**, 2314–2318 (1995).

4. Klotz, S. *et al.* Mechanical unloading during left ventricular assist device support increases left ventricular collagen cross-linking and myocardial stiffness. *Circulation* **112**, 364–374 (2005).
5. Pouleur, H. *et al.* Effects of long-term enalapril therapy on left ventricular diastolic properties in patients with depressed ejection fraction. SOLVD Investigators. *Circulation* **88**, 481–491 (1993).
6. Royse, C.F. & Royse, A.G. The myocardial and vascular effects of bupivacaine, levobupivacaine, and ropivacaine using pressure volume loops. *Anesth. Analg.* **101**, 679–687 (2005).
7. Burkhoff, D., Yue, D.T., Franz, M.R., Hunter, W.C. & Saqawa, K. Mechanical restitution of isolated perfused canine left ventricles. *Am. J. Physiol.* **246**, H8–H16 (1984).
8. Grieve, D.J., Cave, A.C., Byrne, J.A., Layland, J. & Shah, A.M. Analysis of *ex vivo* left ventricular pressure-volume relations in the isolated murine ejecting heart. *Exp. Physiol.* **89**, 573–582 (2004).
9. Regen, D.M., Denton, P.K., Howe, W.C., Taylor, L.K. & Hansen, D.E. Characteristics of left-ventricular isovolumic pressure waves in isolated dog hearts. *Heart Vessels* **9**, 155–166 (1994).
10. Baan, J. *et al.* Continuous measurement of left ventricular volume in animals and humans by conductance catheter. *Circulation* **70**, 812–823 (1984).
11. Little, W.C., Ohno, M., Kitzman, D.W., Thomas, J.D. & Cheng, C.P. Determination of left ventricular chamber stiffness from the time for deceleration of early left ventricular filling. *Circulation* **92**, 1933–1939 (1995).
12. Cecconi, M. *et al.* Doppler echocardiographic evaluation of left ventricular end-diastolic pressure in patients with coronary artery disease. *J. Am. Soc. Echocardiogr.* **9**, 241–250 (1996).
13. Garcia, M.J. *et al.* An index of early left ventricular filling that combined with pulsed Doppler peak E velocity may estimate capillary wedge pressure. *J. Am. Coll. Cardiol.* **29**, 448–454 (1997).
14. Nagueh, S.F. *et al.* Doppler estimation of left ventricular filling pressures in patients with hypertrophic cardiomyopathy. *Circulation* **99**, 254–261 (1999).
15. Neumann, A., Soble, J.S., Anagnos, P.C., Kagzi, M. & Parrillo, J.E. Accurate noninvasive estimation of left ventricular end-diastolic pressure: comparison with catheterization. *J. Am. Soc. Echocardiogr.* **11**, 126–131 (1998).
16. Bohn, J., Rienmüller, R., Seiderer, M. & Strauer, B.E. [Non-invasive determination of the enddiastolic volume of the left ventricle. A comparative angiocardiographic, two-dimensional echocardiographic, computer tomographic and radionuclide ventriculographic study]. *Z. Kardiol.* **72**, 438–447 (1983).
17. Thomsen, J.H. *et al.* Estimation of absolute left ventricular volume from gated radionuclide ventriculograms. A method using phase image assisted automated edge detection and two-dimensional echocardiography. *Chest* **84**, 6–13 (1983).
18. Ichikawa, Y. *et al.* Evaluation of left ventricular volumes and ejection fraction using fast steady-state cine MR imaging: comparison with left ventricular angiography. *J. Cardiovasc. Magn. Reson.* **5**, 333–342 (2003).
19. Chen, C.H. *et al.* Noninvasive single-beat determination of left ventricular end-systolic elastance in humans. *J. Am. Coll. Cardiol.* **38**, 2028–2034 (2001).
20. Senzaki, H., Chen, C.H. & Kass, D.A. Single-beat estimation of end-systolic pressure-volume relation in humans. A new method with the potential for noninvasive application. *Circulation* **94**, 2497–2506 (1996).
21. Shishido, T. *et al.* Single-beat estimation of end-systolic elastance using bilinearly approximated time-varying elastance curve. *Circulation* **102**, 1983–1989 (2000).
22. Klotz, S. *et al.* Single-beat estimation of end-diastolic pressure-volume relationship: a novel method with potential for noninvasive application. *Am. J. Physiol. Heart Circ. Physiol.* **291**, H403–H412 (2006).
23. Mirsky, I. Assessment of passive elastic stiffness of cardiac muscle: mathematical concepts, physiologic and clinical considerations, directions of future research. *Prog. Cardiovasc. Dis.* **18**, 277–308 (1976).
24. Todaka, K. *et al.* Impact of exercise training on ventricular properties in a canine model of congestive heart failure. *Am. J. Physiol.* **272**, H1382–1390 (1997).